N O T I C E

THIS DOCUMENT HAS BEEN REPRODUCED FROM
MICROFICHE. ALTHOUGH IT IS RECOGNIZED THAT
CERTAIN PORTIONS ARE ILLEGIBLE, IT IS BEING RELEASED
IN THE INTEREST OF MAKING AVAILABLE AS MUCH
INFORMATION AS POSSIBLE

Analysis of Starvation Effects on Hydrodynamic Lubrication in Nonconforming Contacts

David E. Brewe
Propulsion Laboratory
AVRADCOM Research and Technology Laboratories
Lewis Research Center
Cleveland, Ohio

and

Bernard J. Hamrock
Lewis Research Center
Cleveland, Ohio

NASA

ANALYSIS OF STARVATION EFFECTS ON HYDRODYNAMIC LUBRICATION

IN NONCONFORMING CONTACTS

by David E. Brewe* and Bernard J. Hamrock

National Aeronautics and Space Administration

Lewis Research Center

Cleveland, Ohio 44135

SUMMARY

Numerical methods were used to determine the effects of lubricant starvation on the minimum film thickness under conditions of a hydrodynamic point contact. Starvation was effected by varying the fluid inlet level. The Reynolds boundary conditions were applied at the cavitation boundary and zero pressure was stipulated at the meniscus or inlet boundary. The analysis is considered valid for a range of speeds and loads for which thermal, piezoviscous, and deformation effects are negligible. It is applied to a wide range of geometries (i.e., from a ball-on-plate configuration to a ball in a conforming groove). Seventy-four cases were used to numerically determine a minimum-film-thickness equation as a function of the ratio of dimensionless load to dimensionless speed for varying degrees of starvation. From this, a film reduction factor was determined as a function of the fluid inlet level. Further, a starved fully flooded boundary was defined and an expression determining the onset of starvation was derived. As the degree of starvation was increased, the minimum film thickness decreased gradually until the fluid inlet level became critical. Reducing the fluid inlet level still further led to a

*Propulsion Laboratory, AVRADCOM Research and Technology Laboratories.

sharp decrease in the minimum film thickness. An expression determining the critically starved fluid inlet level was derived.

The changes in the inlet pressure buildup due to changing the available lubricant supply are presented in the form of three-dimensional isometric plots and also in the form of contour plots. `

INTRODUCTION

The effect of starvation in a hydrodynamically lubricated conjunction can be studied by systematically reducing the inlet supply and observing the resultant pressure distribution and film thickness. This starvation effect can have a significant role in the operation of machine elements. For example, roller-end wear due to roller skewing can be a critical problem for high-speed cylindrical roller bearings. It is desirable that the hydrodynamic film generated between the roller end and the guide flange provide stiffness and damping to limit the amplitude of the roller skewing motion. However, at high rotational speeds the roller end and the flange are often subjected to a depletion in the lubricant supply due to centrifugal effects. In such cases, the minute amount of lubricant available at the roller-end-flange conjunction might well represent an example of steady-state starvation. Starvation effects in hydrodynamically lubricated contacts are important also if one wishes to calculate the rolling and sliding resistance and/or traction encountered in ball and roller bearings (ref. 1). In another example, the effect of restricting the lubricant to a roller bearing is seen experimentally and theoretically to reduce the amount of cage and roller slip (ref. 2). The theoretical analysis was accomplished by changing the location of the boundary where the pressure begins to build up and noting the effect on the hydrodynamic forces. Combining this with relative velocity expressions and equilibrium equations enabled the

determination of the amount of cage and roller slip.

The location of the inlet and exit boundaries as well as the respective boundary conditions to be applied has been one of the most controversial issues concerning starvation of hydrodynamic contacts. The issue of the effect of the lubricant supply on the inlet boundary condition and its consequences to incipient pressure buildup began to materialize as a result of earlier studies applied to rigid cylinders (refs. 3 and 4). Lauder (ref. 5) and Tipei (ref. 6) asserted an upstream limit of the fluid film where the pressure begins to rise as governed by the Reynolds equation. This limit according to Lauder is determined by applying reverse flow boundary conditions (i.e., $u = \partial u / \partial y = 0$). Tipei locates the upstream limit as defined by the line of centers of two bounded vortices that are observed for pure rolling. Both cases have been criticized because their analyses lead to one position of pressure buildup regardless of the oil supply (ref. 7). Dowson (ref. 8), Floberg (refs. 9, 10), and most dramatically, Wedeven, Evans, and Cameron (ref. 11) provide experimental evidence supporting the idea that the location of incipient pressure rise is determined by the oil supply. Further, Wedeven, et al., using a Grubin type of EHD analysis, obtained very good correlation between experiment and the theory of starvation effects by choosing the start of the pressure buildup to occur at the meniscus boundary. Oteri (ref. 12), using stream function analysis for rolling rigid cylinders, showed that incipient pressure rise occurs at the meniscus boundary even in the presence of reverse-flow conditions. In view of this work, starvation effects in machine element applications can be predicted and relied on with a greater degree of confidence.

One of the more important manifestations of lubricant starvation is the

reduction in film thickness. This topic has recieved a good deal of atten-
tion in the literature (refs. 11, 13-21). With the exception of references
13 and 19 to 21, these references are applicable only to elastohydrodynamic
situations. Most of the work concerned with rigid contacts has been devoted
to line contact applications (refs. 13, 20, and 21). Dalmaz and Godet (ref.
19) analyze the effect of the inlet on the film reduction factor for a
sphere against a plate. However, to the authors' knowledge, an effort that
parallels that of Hamrock and Dowson (refs. 14, 15) for the EHD contact is
absent from the rigid contact theory. In those works, an expression was
determined that relates the film reduction to the inlet distance.

The current study is a resumption of a previous rigid-contact analysis
(ref. 22) to extend validity for the minimum-film-thickness equation derived
there over a wider range of film thicknesses as well as to include the
effects of starvation in this equation. The start of the pressure buildup
as determined by the Reynolds equation is assumed to occur at the inlet
meniscus. The location of the cavitation boundary was determined by
applying the Reynolds boundary conditions as discussed in previous work
(ref. 22). The study applies to a wide range of geometries (i.e., from a
ball-on-plate configuration to a ball in a conforming groove). Seventy-four
cases were used to numerically determine (1) an equation relating minimum
film thickness with the fluid inlet level as well as with the dimensionless
load-speed ratio and geometry, (2) an equation predicting the onset of
starvation, and (3) an equation predicting the onset of a critically starved
conjunction. The resulting equations are valid for dimensionless minimum
film thicknesses H_0 ranging from 5.0×10^{-5} to 1.0×10^{-3}. Further,
contour isobar plots and three-dimensional isometric pressure plots are
presented.

C_0, C_1	least-squares coefficients
D	difference, $[(H_0 - \tilde{H}_0)/H_0] \times 100$, percent
H	dimensionless film thickness, h/R_x
H_0	dimensionless minimum (central) film thickness, h_0/R_x
$\tilde{H}_0$	dimensionless calculated minimum (central) film thickness
H_{in}	dimensionless fluid inlet level h_{in}/R_x
H_{in}^*	dimensionless fluid inlet level (onset of starvation)
h	film thickness, m
h_0	minimum (central) film thickness, m
L	reduced hydrodynamic lift, dimensionless
N	direction normal to boundary
P	dimensionless pressure, $pR_x/\eta_0 u$
p	pressure, N/m^2
R	effective radius of curvature, $\dfrac{R_x R_y}{R_x + R_y}$, m
S	separation due to geometry of solids, m
W/U	ratio of dimensionless load to dimensionless speed
u	average surface velocity in x direction, $(u_A + u_B)/2$, m/sec
w	load capacity, N
X	dimensionless coordinate, x/R_x
x	coordinate along rolling direction, m
Y	dimensionless coordinate, y/R_x
y	coordinate transverse to rolling direction, m
α	radius ratio, R_y/R_x
β	film reduction factor

η_0 fluid viscosity at standard temperature and pressure, N sec/m^2

ϕ Archard–Cowking side–leakage factor, $\dfrac{1}{1 + \frac{2}{3a}}$

Subscripts:

A	solid A
B	solid B
cr	critical
f	flooded conjunction
x,y	coordinate direction

NUMERICAL PROCEDURE

The hydrodynamic effects on the central film thickness between two rigid solids in lubricated rolling and/or sliding contact are analyzed under conditions of lubricant starvation. The effects of starvation are determined by systematically decreasing the fluid inlet level. The Reynolds boundary conditions are applied at the cavitation boundary, and zero pressure is stipulated at the meniscus or inlet boundary. The lubricant is assumed to be an incompressible Newtonian fluid under laminar, isothermal, isoviscous, and steady-state conditions. The numerical approach follows that of a previous investigation (ref. 22). There, a fully flooded film profile was specified and a pressure distribution satisfying the Reynolds equation was determined for a given speed, viscosity, and geometry. The analysis treats the two rigid bodies as having parallel principal axes of inertia. This enables one to make a simplifying transformation to an equivalent system of a rigid solid near a plane separated by a lubricant film (fig. 1).

Relevant Equations

The same dimensionless expressions are used here as in reference 22, that is,

$$X = x/R_x, \qquad Y = y/R_x, \qquad H = h/R_x \tag{1}$$

also

$$P = pR_x/\eta_0 u, \qquad \alpha = R_y/R_x$$

The Reynolds equation

$$\frac{\partial}{\partial X}\left(H^3 \frac{\partial P}{\partial X}\right) + \frac{\partial}{\partial Y}\left(H^3 \frac{\partial P}{\partial Y}\right) = 12 \frac{\partial H}{\partial X} \tag{2}$$

is the governing equation within the conjunction.

We recognize that, when the inlet supply levels are increased to values much greater than the minimum film thickness, calculations as governed by the Reynolds equation are inherently in error far from the center of contact. The reason is that the Reynolds equation neglects curvature of the fluid film. Dowson (ref. 23) has pointed out that the errors involved in using this equation to determine the buildup of pressure in such regions are negligible. The predicted pressures are themselves so very much smaller than the effective load-carrying pressures in the region of closest approach of the solids. The dimensionless film thickness equation is given as

$$H = H_0 + 1 - \sqrt{1 - X^2} + \alpha\left[1 - \sqrt{1 - (Y/\alpha)^2}\right] \tag{3}$$

where H is bounded above by the dimensionless fluid inlet level H_{in} and below by the dimensionless minimum film thickness H_0 (i.e., $H_0 \leq H \leq H_{in}$, e.g., fig. 2). The fluid inlet level H_{in} is made dimensionless so that, if the inlet is completely filled, $H_{in} = 1$ and the conjunction is said to be fully flooded.

The Reynolds boundary conditions are used, that is, $P = \partial P / \partial N = 0$ at the cavitation boundary and $P = 0$ at the inlet boundary ($H = H_{in}$). A pressure distribution that satisfies these boundary conditions is then determined numerically by finite differencing. Taking advantage of the fact that the pressure distribution must be symmetric about the direction of motion, only half of the domain was used in the calculations and the other half was determined from symmetry. A variable-mesh nodal structure was used to provide close spacing in and around the pressure peak. This helped to minimize the errors that can occur because of large gradients in the high-pressure region. As before, the integration of the pressure distribution can be used in relating the hydrodynamic effects (i.e., load, speed, and viscosity) to the minimum (central) film thickness for a given fluid inlet level. In general, for a given H_0 and u the load capacity w and/or the dimensionless load-speed ratio is determined as follows:

$$w = \eta_0 u R_x \iint P \, dXdY$$

or

$$W/U = \iint P \, dXdY \tag{4}$$

where $W/U = w/\eta_0 u R_x$.

Fully Flooded Film Thickness

The right side of equation (4) has been shown to be a function of the geometry and the minimum film thickness. For a fully flooded situation ($H_{in} = 1$), equation (4) led to the following relationship in reference 22 (eq. (20)):

$$H_0 = 128 \, a(pUL/W)^2 \qquad \text{for} \qquad 10^{-5} \le H_0 \le 10^{-4} \tag{5}$$

where

$$L = 0.131 \, \tan^{-1}(a/2) + 1.683$$

and

$$\phi = \frac{1}{1 + \frac{2}{3a}}$$

A disadvantage of equation (5) is that it cannot be applied to the full range of dimensionless film thicknesses normally encountered in a rigid contact (i.e., $10^{-5} \leq H_0 \leq 10^{-3}$). Consider, for example, a ball in rolling motion that is loaded against a flat plate. For a load-speed ratio W/U of 340, the numerically determined value (i.e., as determined by finite difference analysis) of the dimensionless film thickness is 10^{-3} (table I). Equation (5) predicts the dimensionless film thickness to be 1.22×10^{-3}, which is in error of the numerical value by 22 percent. Consequently, we wish to revise equation (5) so that it is valid for the thicker films as well. This revised equation should reduce to equation (5) in the limit for thin films. Furthermore, the revised dimensionless film thickness should be expressed in such a way as to easily include the effects of starvation. This would then enable us to present one general expression to be presented for the dimensionless film thickness that can be used for the full range of film thicknesses for a starved conjunction as well as for a fully flooded conjunction. After the numerical analysis for each case was complete, the several curve fits or regression curves of H_0 on W/U were considered that would be consistent with these above requirements. The most suitable curve fit considered was in the form of a more general linear equation (5), that is,

$$\frac{1}{\sqrt{H_0}} = c_1 \frac{W}{U} + c_0 \tag{6}$$

A linear regression by the method of least squares (ref. 24) was performed by using the data ($a = 1.00$) in table I for the fully flooded

condition to determine the constants in equation (6). The coefficient of determination r^2 was found to be 0.999993. The value of r^2 reflects the fit of the data to the resulting equation: 1 being a perfect fit, and 0 being the worst possible fit. The values of C_0 and C_1 are given in table II. It can be verified that in going from equation (5) to equation (6), the coefficient of the load-speed ratio remains unchanged and is entirely a function of geometry, that is,

$$C_1 = \frac{1}{\delta L (128a)^{1/2}} \tag{7}$$

When considering conditions in which the film is thin, it can be shown that C_0 is insignificant to the dimensionless load-speed ratio term, which explains why equation (5) worked so well for the thin-film regime. Using the coefficients C_0, and C_1 as determined above, we can determine the dimensionless film thickness from equation (6) as

$$\bar{H}_{0,f} = \left(\frac{W/U}{\delta L \sqrt{128a}} + 2.6511 \right)^{-2} \tag{8}$$

This expression is valid for the full range of dimensionless film thicknesses normally encountered in a fully flooded undeformed contact.

Generalized Film Thickness Formula (Applicable to
Starved as well as Fully Flooded Conjuctions)

The effect of lubricant starvation on the hydrodynamic film thickness was observed by varying the fluid inlet level to the contact and noting the effect on load capacity for five different film thicknesses for the ball-on-plate contact (i.e., $a = 1.00$). In addition to the fully flooded data, 55 computer-generated data points were used to arrive at a family of equations having the form given in equation (6). An equation for each fluid

inlet level was determined by performing a linear regression by the method of least squares. Table II lists for each fluid inlet level the values of the coefficients C_1 and C_0, the coefficient of determination r^2, and U_{max}, the maximum percentage of error U defined as

$$U = \frac{\bar{H}_0 - H_0}{H_0} \times 100 \tag{9}$$

The table indicates that for all practical purposes, the constant C_1 is again strictly a function of geometry. Furthermore, the entire effect of starvation is represented by the value of C_0 in equation (6). An expression for the coefficient C_0 as a function of the fluid inlet level H_{in} would enable a determination of a generalized minimum-film-thickness formula that applies to starved as well as fully flooded conditions. A close examination of the variation of C_0 with H_{in} in table II reveals that $C_0 \propto (2/H_{in})^{1/2}$ for the severely starved situations. As H_{in} approaches 1, C_0 approaches a value very nearly equal to e (i.e., the base of the natural system of logarithms, 2.718). This suggests $e^{H_{in}}$ as a modulating factor. Further considerations for the nearly flooded inlet levels show that

$$C_0 e^{-H_{in}} \approx [(2 - H_{in})/H_{in}]^{1/2}$$

Finally for the full range of values, C_0 varies with H_{in} as follows:

$$C_0 = k e^{H_{in}} \left(\frac{2 - H_{in}}{H_{in}} \right)^{1/2} \tag{10}$$

where k is a proportionality constant. Equation (10) can be improved by doing an exponential curve fit using the method of least squares on the data $C_0 [H_{in}/(2 - H_{in})]^{1/2}$ with H_{in}. This results in the following equation:

$$c_0 = 1.1137 \ e^{0.8504 \ H_{in}[(2 - H_{in})/H_{in}]^{1/2}} \tag{11}$$

The regression coefficient was 0.9608, indicating a reasonably good fit. By substituting c_1 (eq. (7)) and c_0 (eq. (11)) into equation (6) the minimum film thickness formula becomes

$$\bar{H}_0 = \left[\frac{W/U}{\rho L (128a)^{1/2}} + 1.1137 \left(\frac{2 - H_{in}}{H_{in}} \right)^{1/2} e^{0.8504 \ H_{in}} \right]^{-2} \tag{12}$$

In the interest of simplifying the equation still further, the curve fit constants were rounded off. The round off (i.e., 1.1137 to 1.11, and 0.8504 to 1.0) in this instance actually improved the agreement between H_0 and the actual H_0 in most cases. However, the round off results in a curve fit that is no longer a minimum least squares deviation. Thus, our generalized minimum film thickness formula in terms of geometry (i.e., radius ratio a), load-speed ratio W/U, and fluid inlet level H_{in}, can be written as

$$\bar{H}_0 = \left[\frac{W/U}{\rho L (128a)^{1/2}} + 1.11 \left(\frac{2 - H_{in}}{H_{in}} \right)^{1/2} e^{H_{in}} \right]^{1/2} \tag{13}$$

The measure of agreement between the calculated and input values of H_0 is represented by the value of U (eq. (9)) and presented in table III. Table III shows that, when the fluid inlet level is of the same order of magnitude as the minimum film thickness, the error that results from using equation (13) becomes larger. However, equation (13) can confidently be used for the full range of minimum film thickness if the fluid inlet level is such that $0.004 \leq H_{in} \leq 1.000$. For very thin films (i.e., $H_0 \leq 10^{-4}$) equation (13) can be useful throughout the full range of fluid inlet

levels that were investigated (i.e., $0.001 \leq H_{in} \leq 1.000$). Note that the film thickness formula is intended to be used only for a range of speeds and loads in which piezoviscous and deformation effects are negligible. It was determined that these effects can be significant for minimum film thicknesses less than 5.0×10^{-5}.

Note also from table III that excellent agreement is obtained for the near-line-contact applications (i.e., $\alpha = 36.54$) even though these data were not used in the determination of the above equation (13). Most of the predictions by equation (13) are within 3 percent of the numerically determined values and do not exceed 6 percent for any case.

Equation (13) is equally valid for the fully flooded conjunction as well as for the starved conjunction. That is, if we set $H_{in} = 1.00$, then $\tilde{H}_0 = \tilde{H}_{0,f}$ and equation (13) reduces to

$$\tilde{H}_{0,f} = \left(\frac{W/U}{\phi L \sqrt{128\alpha}} + 3.02\right)^{-2} \tag{14}$$

In comparing this with equation (8), one discrepancy appears. The value of the constant from this equation is slightly different than that determined for equation (8). This comes about, for the most part, from the simplification of the generalized expression (eq. (12)). This difference has not introduced any appreciable error. Table III shows that the error for the full range of minimum film thicknesses investigated (for $H_{in} = 1$) is less than 1 percent for $\alpha = 1$. For the near-line-contact geometry (i.e., $\alpha = 36.54$) the error does not exceed 3.36 percent.

Reduction in Minimum Film Thickness

It is now possible to determine the reduction in minimum film thickness from the fully flooded value if the fluid inlet level is known. This can be done by inserting equation (14) into equation (13), which gives

$$\bar{H}_0 = \left\{ \frac{1}{\sqrt{\bar{H}_{0,f}}} + 3.02 \left[\sqrt{\frac{2 - H_{in}}{H_{in}}} \; e^{(H_{in}-1)} - 1 \right] \right\}^{-2} \tag{15}$$

Dividing both sides of the equation by $\bar{H}_{0,f}$ gives

$$\beta \equiv \frac{\bar{H}_0}{\bar{H}_{0,f}} = \left\{ 1 + 3.02 \; \sqrt{\bar{H}_{0,f}} \left[\sqrt{\frac{2 - H_{in}}{H_{in}}} \; e^{(H_{in}-1)} - 1 \right] \right\}^{-2} \tag{16}$$

where β is the reduction in minimum film thickness due to starvation.

RESULTS AND DISCUSSION

Effect of Starvation on Pressure Distribution

The discussion of lubricant starvation can be facilitated by focusing on one of the simplest geometric arrangements (i.e., a ball rolling and/or sliding against a flat plate) as shown in figure 2. The figure compares the pressure distribution determined numerically for the fully-flooded inlet with the most severely starved inlet ($H_{in} = 0.001$). The comparison is made for a constant minimum film thickness (i.e., $H_0 = 1.0 \times 10^{-4}$). Note that the pressure peak built up in the starved inlet is only slightly smaller than that of the fully flooded inlet. However, the area of pressure build-up is considerably smaller, and so the starved inlet is unable to support as much load for a given film thickness as the fully-flooded inlet.

Figure 3 provides the same sort of comparison but for a thicker minimum film (i.e., $H_0 = 1.0 \times 10^{-3}$). The significant difference between the two figures is that the starved inlet for the thicker film has a more pronounced effect on the pressure peak. The fluid inlet level ($H_{in} = 0.002$) for the thicker film represents a relatively more highly starved inlet since H_{in}

14

is of the order of H_0 in this case. The other feature to be noticed in comparing figures 2 and 3 is that the pressure distribution is more evenly spread out for the thicker film. Thus, changes in the meniscus (or integration domain) are going to have a more noticeable effect on the load-carrying capacity. Note also that because of the boundary conditions the integration domain takes on a "kidney-shaped" appearance. This is more clearly shown in the isobaric contour plot shown in figure 4.

Minimum Film Thickness Equation

Thus far we have compared the pressure build up in a severely starved inlet with that in a fully flooded inlet for two minimum film thicknesses. Our investigation, however, included several fluid inlet levels for a variety of minimum film thicknesses. The results are summarized in table III.

A generalized minimum film thickness formula (eq. (13)) was derived from the results of table III. Figure 5 indicates how well the equation represents the computer generated data in the table. It was not possible to display all these results in figure 5. However, the figure is representative of the overall results. The equation fits the data quite well except when the fluid inlet level is of the same order of magnitude as the minimum film thickness. Based on the discussion concerning peak pressure, it would seem that the formula holds well for those cases in which the degree of starvation is such that peak pressure is not significantly reduced.

Of course, it would be most desirable to compare the data in table III with experimental data. To the authors' knowledge, the only available experimental data were obtained by Dalmaz and Godet (ref. 25). To compare equation (13) with experiment, the data from reference 25 were replotted in

figure 6. The experimental data were taken under lightly loaded (rigid contact), isoviscous conditions for pure sliding of a ball on a plate. The fluid inlet level in these experiments was reported to be 1 millimeter. The ball diameter was 30 millimeters; consequently the dimensionless fluid inlet level H_{in} was 0.067. The experimental data were presented as a plot of the dimensionless parameters H_0/WG versus $U/W^{1.5}G^{0.5}$. The materials parameter G in the plot was included so as to accomodate the elastohydrodynamic range in a more general way.

Here, we wish to compare our hydrodynamic starvation theory only with the hydrodynamic results of Dalmaz and Godet. To do this, the ordinate and abscissa were properly scaled (assuming a reasonable value of $WG = 4.5 \times 10^{-4}$) so that the minimum film thickness could be plotted against the dimensionless load-speed ratio as shown in figure 6. The solid line in figure 6 is a plot of equation (13) for $\alpha = 1$ and $H_{in} = 0.067$. The dashed line represents a previous theory (ref. 22) in which the reduced inlet level due to starvation was not considered. The present theory (eq. (13)) shows better agreement with the experimental results than our previous theory (ref. 2) for lower values of W/U. This is because under conditions of low load and/or high speed, the pressures become more significant away from the center of the contact. Consequently, neglecting the size of the inlet introduces an increasing amount of error as W/U is decreased.

Although consideration of the size of the inlet domain improves the agreement of the theory with experiment for the thicker films, still further improvement is possible. It is believed that the effects of reverse flow in the inlet must be included in the theory to obtain better agreement. If reverse flow is considered, not all the available lubricant determined by the fluid inlet level will pass through the contact. The hydrodynamic

contact would essentially see this as a reduction in supply from what actually is there. In other words, the inlet is more severely starved than we have taken into account. From figure 5, we see that increasing the severity of starvation has more effect on the load capacity for thicker films (i.e., $H_0 = 10^{-3}$) than it does for thinner films (i.e., $H_0 = 10^{-4}$). Consequently, reverse-flow considerations should improve agreement between theory and experiment for the thicker films while still maintaining good agreement in the thin-film range.

Lubricant Film Thickness Reduction Factor and Onset of Starvation

Of practical importance to lubricant starvation is the reduction in minimum film thickness β from the fully flooded value. Equation (16) is a derived expression for β in terms of the fluid inlet level and the fully flooded film thickness (also given by eq. (14)). Figure 7 is a plot of β as a function of the fluid inlet level H_{in} for several values of $\tilde{H}_{0,f}$. It is of interest to determine a fully flooded – starved boundary (i.e., that fluid inlet level after which any further decrease causes a significant reduction in the film thickness). Hamrock and Dowson (ref. 14) determined this boundary for elastohydrodynamic (EHD) applications upon satisfying the following condition:

$$1 - \beta \big|_{H_{in} = H_{in}^*} = 0.031 \tag{17}$$

The value of 0.03 was used in equation (17) since it was ascertained that the data in table I were accurate to only ±3 percent.

Thus, for a given value of $\tilde{H}_{0,f}$, one can solve for a value of H_{in}^* that satisfies equation (17). A suitable relationship between H_{in}^* and $\tilde{H}_{0,f}$ can be obtained by generating a table of values (e.g., table IV) and fitting a power curve by the method of least squares. This gives

$$H^*_{in} = 4.11 \left(\bar{H}_{0,f} \right)^{0.36} \tag{18}$$

Thus, we have an equation that determines the onset of starvation. That is, for $H_{in} \geq H^*_{in}$ a fully flooded condition exists, whereas for $H_{in} < H^*_{in}$ a starved condition exists.

Critically Starved Inlet

In certain bearing applications, the power loss resulting from churning of the oil may be higher than the power loss resulting from friction of the bearing alone (ref. 26). These power losses can be minimized by reducing the lubricant supply until a loss in film thickness causes the friction losses to increase. According to the results shown in figure 7, the fluid inlet level can be decreased substantially without adversely affecting the minimum film thickness. Consequently, it might be advantageous to operate the bearing with a lubricant supply just sufficient to preclude any drastic reductions in minimum film thickness, as seen in the figure. Such a critical fluid inlet level might well be defined to occur at the knee of the curve, that is,

$$\left. \frac{d(\beta)}{dH_{in}} \right|_{H_{in}=H_{in,cr}} = 1 \tag{19}$$

Solutions to this expression for several values of minimum film thickness are listed in table IV. A power curve fit by the method of least squares gives

$$H_{in,cr} = 0.8754 \left(H_{0,f} \right)^{0.2977} \tag{20}$$

The regression coefficient for this fit was determined to be 0.9999, indicating an extremely good fit.

CONCLUDING REMARKS

Numerical methods were used to determine the effects of lubricant starvation on the minimum film thickness under conditions of hydrodynamic point contact. Starvation was effected by varying the fluid inlet level. The Reynolds boundary conditions were applied at the cavitation boundary, and zero pressure was stipulated at the meniscus or inlet boundary. The analysis is considered valid for a range of speeds and loads for which thermal, piezoviscous, and deformation effects are negligible. It can be applied to a wide range of geometries (i.e., from a ball-on-plate configuration to a ball in a conforming groove). Seventy-four cases were used to numerically determine

(1) A generalized expression for the minimum film thickness as a function of dimensionless load-speed ratio, geometry, and fluid inlet level (eq. (13)). The expression should be applied for film thicknesses in the range $1.0 \times 10^{-3} \geq H_0 \geq 1.0 \times 10^{-4}$ and for fluid inlet levels of $0.004 \leq H_{in} \leq 1.00$. For $5 \times 10^{-5} \leq H_0 \leq 10^{-4}$ the equation can be applied for a fluid inlet level of $0.001 \leq H_{in} \leq 1.00$.

(2) A film thickness reduction factor (eq. (16)) expressed as a function of the degree of starvation (or fluid inlet level) for a given fully flooded film thickness value.

(3) An equation (eq. (18)) that determines the onset of starvation.

(4) An equation (eq. (20)) that determines a critically starved contact. Contour isobar plots and three-dimensional isometric plots are also presented.

REFERENCES

1. Chiu, Y. P.: A Theory of Hydrodynamic Friction Forces in Starved Point Contact Considering Cavitation. J. Lubr. Technol., vol. 96, no. 2, Apr. 1974, pp. 237-246.

2. Boness, R. J.: The Effect of Oil Supply on Cage and Roller Motion in a Lubricated Roller Bearing. J. Lubr. Technol., vol. 92, no. 1, Jan. 1970, pp. 39-53.

3. Martin, H. M.: The Lubrication of Gear-Teeth. Engineering (London), vol. 102, 1916, pp. 119-121.

4. Peppler, W.: Druckuebertragung and Geschmierten Zylindrischen Gleit- und waelzflaechen. V.D.I. Forschung. 1938, p. 391, Supp. to Forschung auf dem Gebiete des Ingenieurwesens, vol. 9, no. 4, July - Aug. 1938.

5. Lauder, W.: Hydrodynamic Lubrication of Proximate Cylindrical Surfaces of Large Relative Curvature. Proc. Instn. Mecn. Eng., vol. 180, pt. 3B, 1965-66, pp. 101-106.

6. Tipei, N.: Boundary Conditions of a Viscous Flow Between Surfaces with Rolling and Sliding Motion. J. Lubr. Technol., vol. 90, no. 1, Jan. 1968, pp. 254-261.

7. Saman, W. Y.: A Study of Starved Elastohydrodynamic Lubrication with Particular Reference to Gyroscope Bearings. Ph.D. Thesis, Inst. of Tribology, Leeds University, July 1974, p. 25.

8. Dowson, D.: Laboratory Experiments and Demonstrations in Tribology; No. 2 - The Principles of Hydrodynamic Lubrication. Tribology, vol. 1, no. 2, Mar. 1968, pp. 104-108, and vol. 1, no. 3, Aug. 1968, pp. 150-156.

9. Floberg, L.: On Hydrodynamic Lubrication with Special Reference to Sub-cavity Pressures and Number of Streamers in Cavitation Regions. Acta. Polytech. Scand., Ser. ME. 19, 1965.

10. Floberg, L.: Lubrication of Two Rotating Cylinders at Variable Lubricant Supply with Reference to the Tensile Strength of the Liquid Lubricant. J. Lubr. Technol., vol. 95, no. 2, Apr. 1973, pp. 155-165.

11. Wedeven, L. D.; Evans, D.; and Cameron, A.: Optical Analysis of Ball Bearing Starvation. J. Lubr. Technol., vol. 93, no. 3, July 1971, pp. 349-363.

12. Oteri, B. I.: A Study of the Inlet Boundary Condition and the Effect of Surface Quality in Certain Lubrication Problems. Ph.D. Thesis, Leeds University, 1972.

13. Wolveridge, P. E.; Baglin, K. P.; and Archard, J. F.: The Starved Lubrication of Cylinders in Line Contact. Proc. Instn. Mech. Eng., vol. 185, 81/71, 1970/1971, pp. 1159-1169.

14. Hamrock, B. J.; and Dowson, D.: Isothermal Elastohydrodynamic Lubrication of Point Contacts, Part IV – Starvation Results. J. Lubr. Technol., vol. 99, no. 1, Jan. 1977, pp. 15-23.

15. Hamrock, B. J.; and Dowson, D.: Elastohydrodynamic Lubrication of Elliptical Contacts for Materials of Low Elastic Modulus, II – Starved Conjunction. J. Lubr. Technol., vol. 101, no. 1, Jan. 1979, pp. 92-98.

16. Orcutt, F. K.; and Cheng, H. S.: Lubrication of Rolling-Contact Instrument Bearings. Proceedings of the Gyro-Spin Axis Hydrodynamic Bearing Symposium, Vol 2: Ball Bearings, Massachusetts Institute of Technology, 1966.

17. Castle, P.; and Dowson, D.: A Theoretical Analysis of the Starved Elastohydrodynamic Lubrication Problem for Cylinders in Line Contact. Elastohydrodynamic Lubrication, Institution of Mechanical Engineers, (London), 1972, pp. 131-137.

18. Wymer, D. G.; and Cameron, A.: Elastohydrodynamic Lubrication of a Line Contact. Proc. Instn. Mech. Eng., (London) vol. 188, no. 19/74, 1974, pp. 221-238.

19. Dalmaz, G.; and Godet, M.: Effets des Conditions d'Alimentation sur l'Epaisseur du Film dans les Contacts Hertziens Lubrifies. Mec. Materiaux Elec. (France) no. 296-297, Aug.-Sept. 1974, pp. 25-34. (See NASA TM-75782, 1980, for Transl.)

20. Floberg, L.: Lubrication of a Rotating Cylinder on a Plane Surface, Considering Cavitation. Trans. Chalmers Univ. Techn., (Gothenburg), no. 216, 1959.

21. Floberg, L.: Lubrication of Two Cylindrical Surfaces, Considering Cavitation. Trans. Chalmers Univ. Techn., (Gothenburg), no. 234, 1961.

22. Brewe, D. E.; Hamrock, B. J.; and Taylor, C. M.: Effect of Geometry on Hydrodynamic Film Thickness. J. Lubr. Technol., vol. 101, no. 2, Apr. 1979, pp. 231-239.

23. Dowson, D.: The Inlet Boundary Condition. Cavitation and Related Phenomena in Lubrication, D. Dowson, M. Godet, and C. M. Taylor, eds., Mechanical Engineering Publications, Ltd., 1975, pp. 143-152.

24. Spiegel, Murray R.: Schaum's Outline of Theory and Problems of Statistics. McGraw-Hill, 1961.

25. Dalmaz, G.; and Godet, M.: Traction, Load, and Film Thickness in Lightly Loaded Lubricated Point Contacts. J. Mech. Eng. Sci., vol. 15, no. 6, Dec. 1973, pp. 400-409.

26. Styri, H.: Friction Torque in Ball and Roller Bearings. Mech. Eng., vol. 62, no. 12, Dec. 1940, pp. 886-890.

TABLE I. - DATA SHOWING EFFECT OF STARVATION ON DIMENSIONLESS LOAD-SPEED

RATIO FOR FIVE VALUES OF MINIMUM FILM THICKNESS

[Average surface velocity in x-direction, u, 10 cm/sec; fluid viscosity, η_0, 0.411x10^{-5} N sec/cm^2; effective radius of curvature, R_x, 1.11125 cm.]

Dimensionless fluid inlet level, H_{in}	Dimensionless minimum film thickness, H_0					
	1×10^{-5}	5×10^{-5}	1×10^{-4}		5×10^{-4}	1×10^{-3}
	Radius ratio, a					
	1.0	1.0	1.0	36.53	1.0	1.0
	Dimensionless load-speed ratio, W/U					
1.000	3706.19	1646.74	1153.59	12430.92	495.54	339.57
.750	3705.64	1646.27	1153.04	12428.08	495.03	339.07
.500	3703.28	1643.91	1150.63	12403.77	492.67	336.69
.250	3695.02	1635.68	1142.56	12323.86	484.56	328.74
.150	3685.41	1626.05	1132.67	12224.01	474.73	318.45
.070	3665.43	1606.16	1106.40	12042.07	453.65	295.66
.035	3646.44	1570.61	1077.98	11552.18	421.79	265.78
.020	3613.91	1536.33	1044.01	11169.70	387.20	234.64
.010	3552.69	1474.84	982.80	10503.93	332.44	184.46
.004	3447.63	1372.16	862.57	9232.69	232.77	89.74
.002	3294.44	1221.52	735.61	7869.48	127.97	25.95
.001	3108.58	1041.53	567.75	6127.10	37.08	a4.53

aThis value of W/U was determined by using $H_0 = 7.5 \times 10^{-4}$, since $H_0 = 1 \times 10^{-3}$ results in no load capacity.

TABLE II. - CONSTANTS APPEARING IN FILM THICKNESS EQUATION

(EQ. (6)) FOR EACH FLUID INLET LEVEL

Dimensionless fluid inlet level, H_{in}	Least-squares coefficients		Coefficient of determination, r^2	Maximum percentage of error in film thickness determination (eq. (9)), v_{max}
	c_1	c_0		
1.000	0.08455	2.6511	0.99999	+1.67
.750	.08455	2.6931		+1.67
.500	.08455	2.8941		+1.67
.250	.08456	3.5720		+1.61
.150	.08454	4.4226		+1.78
.070	.08447	6.3850		+1.68
.035	.08414	9.2635	1.00000	-0.14
.020	.08418	12.0388	1.00000	-1.06
.010	.08440	16.6239	.99999	-3.51
.004	.08452	25.2892	.99990	-7.47
.002	.08630	33.5023	.99934	-21.72
.001	.08878	43.2636	.99737	-30.07

TABLE III. - COMPARISON OF DIMENSIONLESS FILM THICKNESS VALUES FROM EQUATION (13) WITH DIMENSIONLESS FILM THICKNESS VALUES INPUT TO COMPUTER
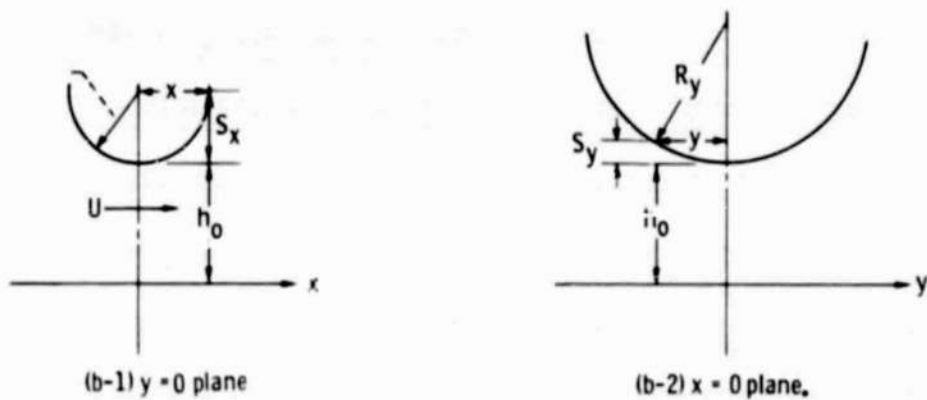
This value of H^*_{in} was determined using $H_0 = 7.5 \times 10^{-4}$, since $H_0 = H^*_{in}$ results in no load capacity.

TABLE IV. - DIMENSIONLESS FLUID INLET VALUES THAT DETERMINE STARVED -

FULLY FLOODED BOUNDARY AND CRITICALLY STARVED BOUNDARY FOR SEVERAL

VALUES OF MINIMUM FILM THICKNESS FOR A FLOODED CONJUNCTION

Dimension-less fluid inlet values	Dimensionless minimum film thickness, for a flooded conjunction, $H_{0,f}$						
	5×10^{-5}	7.5×10^{-5}	1×10^{-4}	2.5×10^{-4}	5×10^{-4}	7.5×10^{-4}	1×10^{-3}
H^*_{in}	0.107	0.130	0.148	0.212	0.265	0.297	0.320
$H_{in,cr}$	.046	.052	.056	.074	.091	.103	.112

(a-1) y = 0 plane.

(a-2) x = 0 plane.

(a) Two rigid solids separated by a lubricant film.
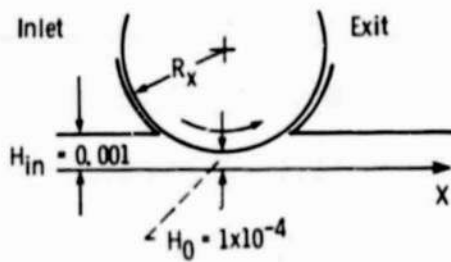
(b-1) y = 0 plane

(b-2) x = 0 plane.

(b) Equivalent system of a rigid solid near a plane separated by a lubricant film.
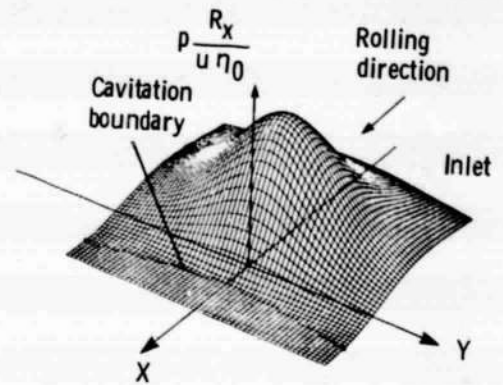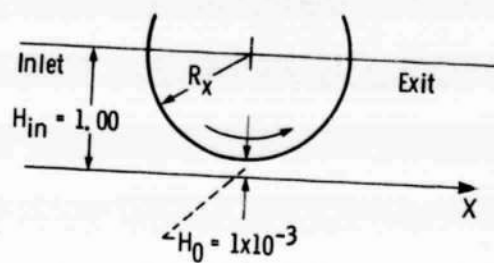
Figure 1. - Contact geometry.
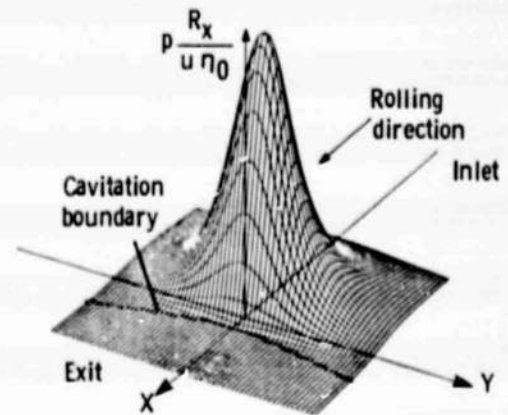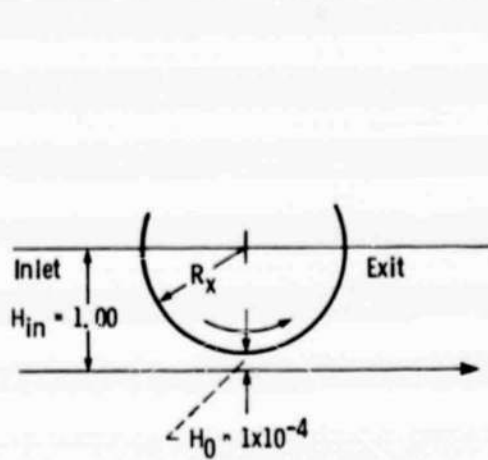
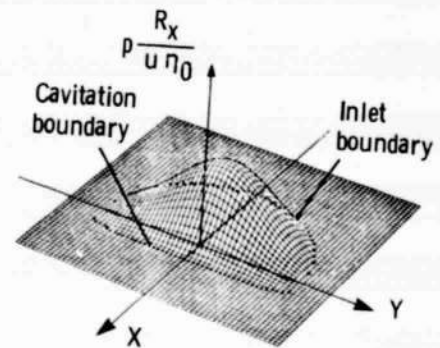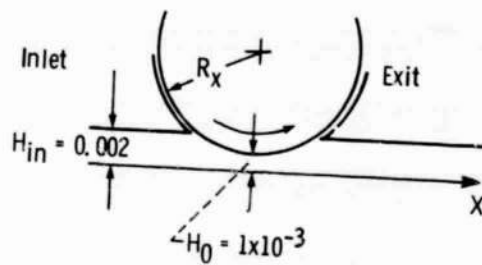(a) Fully flooded condition: dimensionless fluid inlet level $H_{in} = 1.00$.
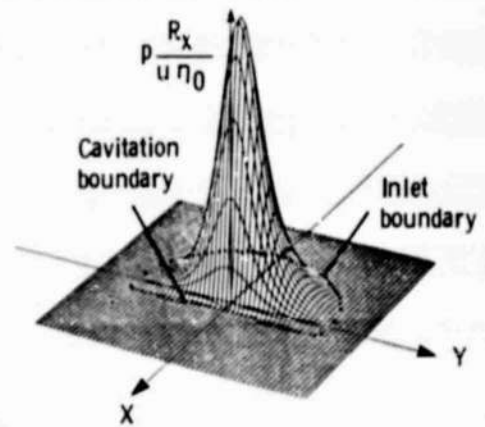
(b) Starved condition: dimensionless fluid inlet level $H_{in} = 0.001$.

Figure 2. - Three-dimensional representation of pressure distribution, comparing starved with fully flooded conjunction for dimensionless minimum film thickness $H_0 = 1 \times 10^{-4}$.
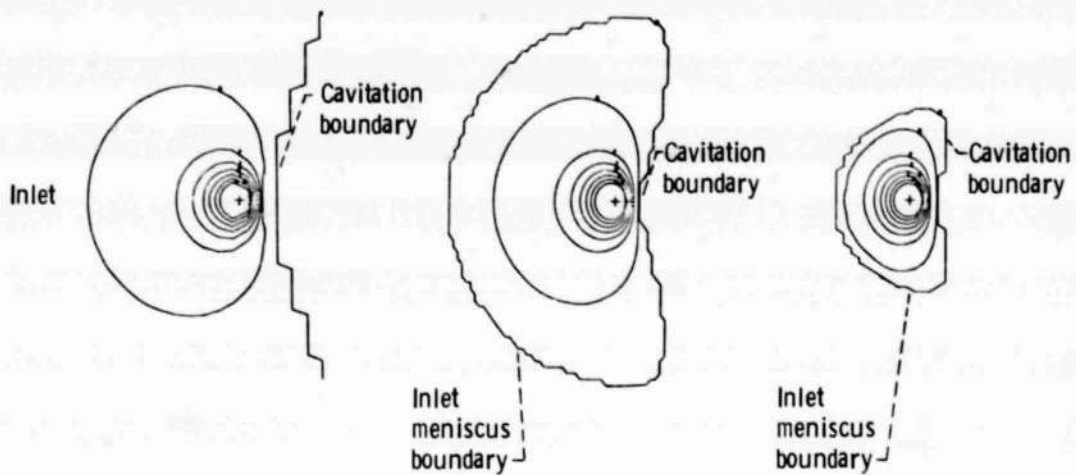
(a) Fully flooded condition: dimensionless fluid inlet level $H_{in} = 1.00$.

(b) Starved condition: dimensionless fluid inlet level $H_{in} = 0.002$.

Figure 3. - Three-dimensional representation of pressure distribution, comparing starved with fully flooded conjunction for dimensionless minimum film thickness $H_0 = 1 \times 10^{-3}$.

(a) Fully flooded condition: dimensionless fluid inlet level $H_{in} = 1.00$; dimensionless maximum pressure $P_{max} = 1.20 \times 10^6$; dimensionless load-speed ratio $W/U = 1153.6$.

(b) Starved condition: $H_{in} = 0.004$; $P_{max} = 1.19 \times 10^6$; $W/U = 862.6$.

(c) Starved condition: $H_{in} = 0.001$; $P_{max} = 1.13 \times 10^6$; $W/U = 567.8$.

Figure 4. - Isobaric contour plots for three fluid inlet levels for dimensionless minimum film thickness $H_0 = 1 \times 10^{-4}$.

Dimensionless fluid inlet level,
H_{in}

○	1.000
◇	.035
▽	.010
□	.004
△	.002
▷	.001
——	Eq. (13)

$$\tilde{H}_0 = \left[\frac{W/U}{\varphi L \, (1.28\alpha)^{1/2}} + 1.11 \left(\frac{2 - H_{in}}{H_{in}} \right)^{1/2} e^{H_{in}} \right]^{-2}$$
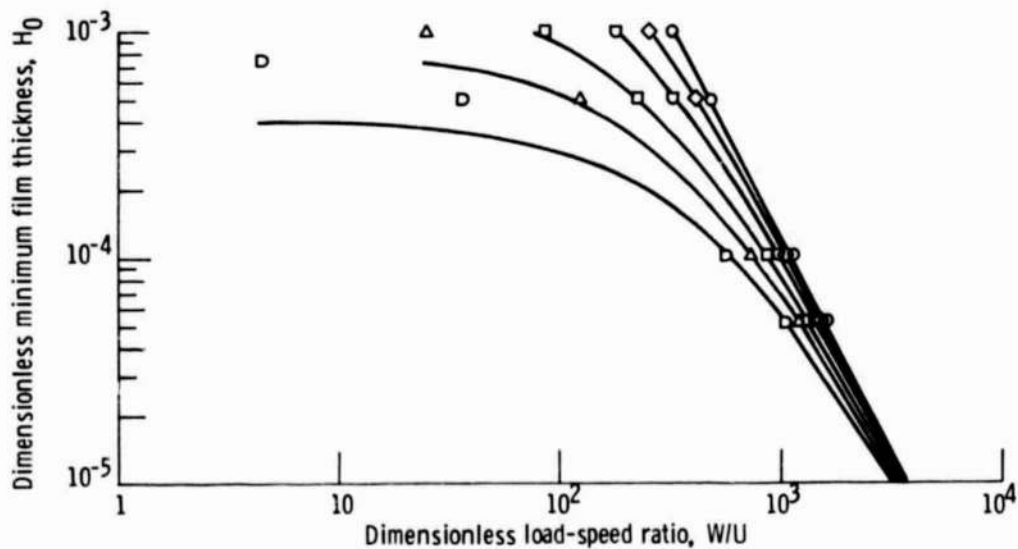

Figure 5. - Comparison of dimensionless minimum film thickness equation (eq. (13)) with computer-generated data as a function of dimensionless load-speed ratio for several values of dimensionless fluid inlet level.
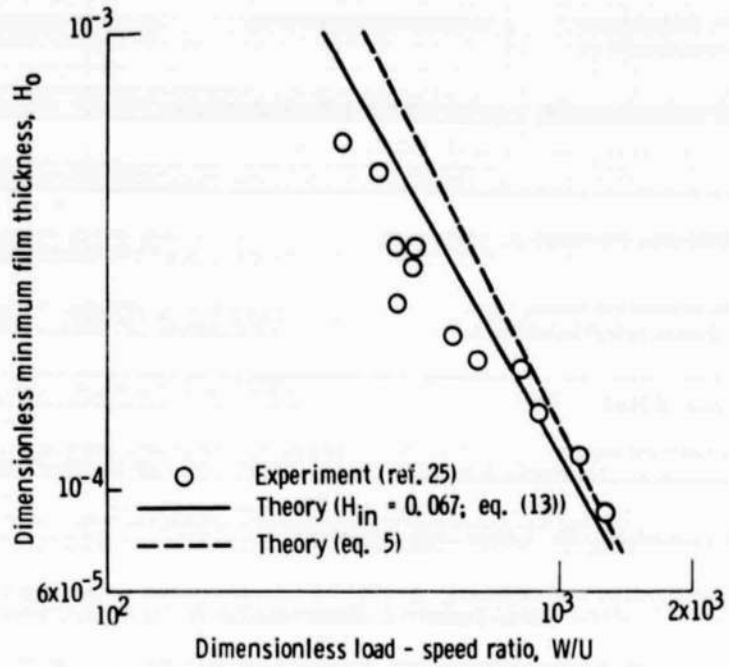
Figure 6. - Theoretical and experimental results.

$$\beta \equiv \frac{\tilde{H}_0}{H_{0,f}} = \left\{ 1 + 3.02 \sqrt{H_{0,f}} \left[\sqrt{\frac{2 - H_{in}}{H_{in}}} e^{(H_{in} - 1)} - 1 \right] \right\}^{-2}$$
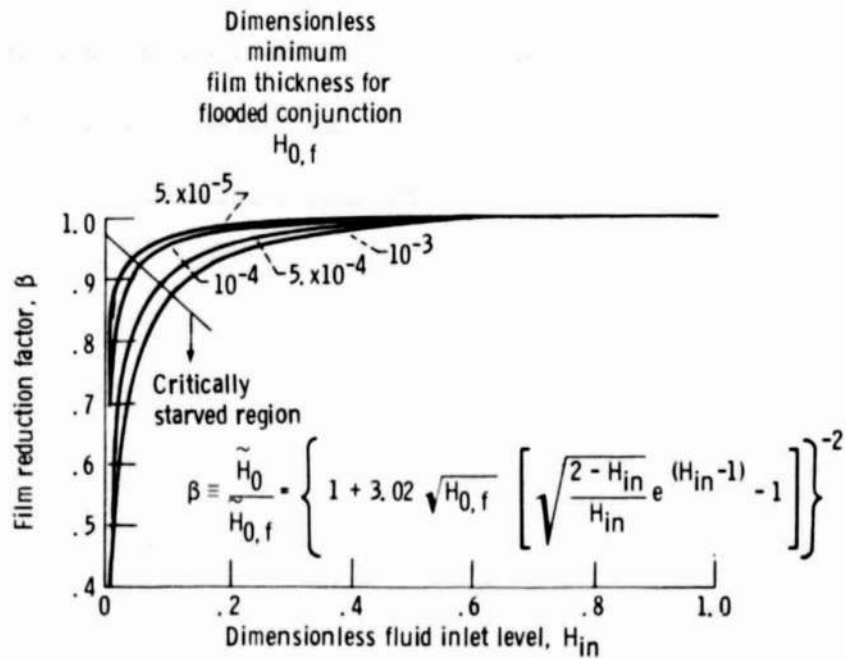
Figure 7. - Minimum film thickness reduction factor as a function of fluid inlet level for several values of dimensionless minimum film thickness for flooded conjunction.